Inorganic Chemistry

Article

pubs.acs.org/IC

Copper(I) Complexes Based on Five-Membered P^N Heterocycles: Structural Diversity Linked to Exciting Luminescence Properties

Daniel M. Zink,[†] Thomas Baumann,*[,†] Jana Friedrichs,[†] Martin Nieger,[‡] and Stefan Bräse*[,§,⊥]

[†]Cynora GmbH, Hermann-von-Helmholtz-Platz 1, D-76344 Eggenstein-Leopoldshafen, Germany

[‡]Laboratory of Inorganic Chemistry, Department of Chemistry, University of Helsinki, P.O. Box 55 (A.I. Virtasenaukio 1), FIN-00014 University of Helsinki, Finland

[§]Institute of Organic Chemistry, Karlsruhe Institute of Technology, KIT Campus South, Fritz-Haber-Weg 6, D-76131 Karlsruhe, Germany

[⊥]Karlsruhe Institute of Technology (KIT), Institute of Toxicology and Genetics, Hermann-von-Helmholtz-Platz 1, D-76344 Eggenstein-Leopoldshafen, Germany

Supporting Information

ABSTRACT: Bridging P^N ligands bearing five-membered heterocyclic moieties such as tetrazoles, 1,2,4-triazoles, oxadiazoles, thiadiazoles, and oxazoles have been investigated regarding their complexation behavior with copper(I) iodide as metal salts. Different complex structures were found, depending either on the ligand itself or on the ligand-to-metal ratios used in the complexation reaction. Two different kinds of luminescent dinuclear complex structures and a kind of tetranuclear complex structure were revealed by X-ray single-crystal analyses and were further investigated for their photophysical properties. The emission maxima of these complexes are in the blue to yellow region of the visible spectrum for the dinuclear complexes and in the yellow to orange region for the tetranuclear complexes. Further investigations using density functional theory (DFT) show that the highest occupied molecular orbital (HOMO) is located mainly on the metal halide cores, while the lowest unoccupied molecular orbital (LUMO) resides mostly in the ligand sphere of the complexes. The emission properties were further examined in different environments such as neat powders, neat films, PMMA matrices, or dichloromethane solutions, revealing the high potential of these complexes for their application in organic light-emitting diodes. Especially complexes with 1,2,4-triazole moieties feature emission maxima in the blue region of the visible spectrum and quantum yields up to 95% together with short decay times of about 1−4 μs and are therefore promising candidates for blue-emitting materials in OLEDs.

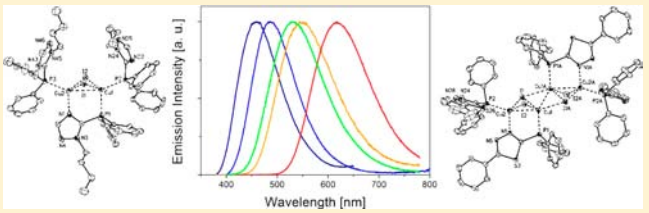

INTRODUCTION

A great deal of research has focused on the development of new concepts for light and display applications and for energy-generating concepts based on organic electronics.[1−12] Luminescent metal complexes based on Ir, Pt, and Os are promising candidates for applications as emitting materials in organic light-emitting devices, because of their color tunability and their high efficiencies.[13−32] However, since these emitting materials are based on rare and expensive metals, luminescent complexes based on more abundant d^{10} metals such as Cu(I), Ag(I), and Au(I) have been brought to the forefront of current research.[33−37] Copper complexes offer exciting photoluminescence characteristics along with a high structural diversity and, furthermore, have been successfully tested as emitting compounds in organic light-emitting devices during the last few years.[38−60] A large number of mono-, di-, tri-, and tetranuclear copper(I) complexes are known, and their formation often depends on the nature of the ligand used for complexation, i.e. whether it is monodentate, bidentate (chelating or bridging), or tridentate, as well as the ligand-to-metal ratio used for the complexation reaction.[54,61−72] For example, recently reported 1,2,3-triazole-based ClickPhos-type ligands and copper(I) halides form di-, tri-, and tetranuclear complexes depending on the substitution pattern of the ligand and on the solvent used for synthesis or for the recrystallization of these kinds of complexes.[39]

Within a given system, colors can be tuned by changing the electronic characteristics of the ligands. This has been shown previously for mononuclear,[56,57,73] dinuclear,[42,67] trinuclear,[39] and tetranuclear[74] systems and was also recently reported by our group for a dinuclear complex with a butterfly-shaped copper(I) halide core and three ligands in the ligand sphere with one ligand acting as a bridging unit and two ligands coordinating via their phosphorus atoms.[38] In this system, it was possible to shift the emission maximum from the blue to the red region of the visible spectrum by changing the electronic characteristics of the ligands used for complexation.

Received: July 24, 2013
Published: November 8, 2013

A direct correlation between the energy of the lowest unoccupied molecular orbital (LUMO) of the ligand and that of the complex was found using DFT calculations: the LUMO energy of the complex is typically localized on the ligand, while the HOMO is localized on the metal centers. Therefore, by changing the electronic structure of the ligand to increase its LUMO energy, the HOMO−LUMO gap consequently increases. Those complexes were based on P^N ligands with substituted pyridine moieties. However, pyridines are known to be electron-poor heterocycles. Strong electron donor substituents were needed in order to shift the emission maximum into the blue region of the visible spectrum. In contrast, five-membered heterocycles are generally known to be electron-rich heterocycles with high-lying LUMO energies,[75] and therefore should be well suited for complexes with emission maxima in the blue range of the visible spectra. The aim of this study was the investigation of P^N ligands with different five-membered heterocycles in order to obtain deep blue emitting complexes.

EXPERIMENTAL SECTION

General Procedures. All reactions were performed in oven-dried glassware under a nitrogen atmosphere. Solvents and chemicals used were purchased from commercial suppliers. Solvents were dried under standard conditions. All materials were used without further purification. Thin-layer chromatography (TLC) was carried out on silica gel plates (silica gel 60, F254, Merck) with detection by UV. Purification was performed with preparative chromatography using normal-phase silica gel (silica gel 60, 230−400 mesh, Merck). ^{1}H NMR, ^{13}C NMR, and ^{31}P NMR spectra were recorded on a Bruker AM 400 or Bruker DRX 250 instrument, respectively. Chemical shifts are reported as δ values (ppm). The signal abbreviations are as follows: s, singlet; bs, broad singlet; d, doublet; t, triplet; q, quartet; quin, quintet; m, multiplet; Ar−H, aromatic proton. The signals of ^{13}C NMR spectra were assigned through DEPT (distortionless enhancement by polarization transfer) technology. The signal abbreviations are as follows: C−Ar, aromatic carbon; +, primary or tertiary carbon; −, secondary carbon; C_{quat}, quaternary carbon. MS (EI) (electron impact mass spectrometry), FAB (fast atom bombardment mass spectrometry), and HRMS (high resolution mass spectrometry) were carried out on a Finnigan MAT 90 instrument (70 eV). The molecular fragments are quoted as the relation between mass and charge (m/z) and the intensities as percentage values relative to the intensity of the base signal (100%). The abbreviation [M$^+$] refers to the molecular ion. Descriptions without nominated temperature were done at room temperature, and the following abbreviations were used: calcd, theoretical value; found, measured value. Information is given in mass percent. IR (infrared spectroscopy) was carried out on a Bruker IFS 88 FT-IR instrument. IR spectra of solids were recorded in KBr and as thin films on KBr for oils and liquids. The deposit of the absorption band was given in wavenumbers $\tilde{\nu}$ in cm^{-1}. The forms and intensities of the bands were characterized as follows: s, strong (10−40% transmission); m, medium (40−70% transmission); w, weak (70−90% transmission); vw, very weak (90−100% transmission); br, broad.

Synthesis of P^N-Type Ligands. Spectroscopic data of ligand **5**[76] have already been reported; for spectroscopic data of ligands **1**−**4** and **6**−**8** refer to the Supporting Information. Precursors **14** and **15** were synthesized following the procedures reported by Kawano et al.[77] Precursor **16** was synthesized according to a reaction sequence reported by Gierczyk et al.,[78] and the tetrazole precursor **18** was obtained following a reaction reported by Vorobiov et al.[79]

*General Procedure for the Alkylation of 1,2,4-Triazoles Yielding Compounds **10**−**13**.*[80] A solution of diazabicycloundecene (52.1 mmol, 1.20 equiv) in tetrahydrofuran (10 mL) was added dropwise to a solution of 1*H*-1,2,4-triazole (43.4 mmol, 1.00 equiv) and the appropriate alkyl halide (47.7 mmol, 1.10 equiv) under a nitrogen atmosphere at room temperature. The reaction mixture was stirred for 24 h at room temperature and subsequently quenched with water (50 mL). The aqueous layer was extracted with dichloromethane (3 × 80 mL). Afterward the organic layers were combined, washed with brine (80 mL), and dried over $MgSO_4 \cdot H_2O$ and the solvent was removed under vacuum. The crude products were used without further purification.

*General Procedure for the Phosphorylation of Alkylated Compounds **10**−**13** Yielding Compounds **1**−**4**.* The alkylated triazole precursor (21.6 mmol, 1.00 equiv) was dissolved in dry tetrahydrofuran (20 mL) under a nitrogen atmosphere and cooled to −80 °C. Lithium diisopropylamine (1.8 M in tetrahydrofuran, 23.8 mmol, 1.10 equiv) was added to this solution dropwise via cannula. The reaction mixture was warmed to 0 °C and was subsequently cooled to −80 °C again. Chlorodiphenylphosphane (22.7 mmol, 1.05 equiv) dissolved in tetrahydrofuran (10 mL) was added dropwise via cannula, and the mixture was warmed to room temperature overnight. After quenching with water (2 mL), the mixture was filtered through a plug of silica gel. The product was obtained by purification via flash column chromatography.

*General Procedure for the Synthesis of Compounds **5**−**7**.* The appropriate oxadiazole or thiadiazole precursor (20.5 mmol, 1.00 equiv) and triethylamine (205 mmol, 10.0 equiv) were dissolved in pyridine (40 mL) under a nitrogen atmosphere. Chlorodiphenylphosphane (30.8 mmol, 1.50 equiv) was added dropwise to this solution at room temperature. The reaction mixture was stirred for 24 h and subsequently quenched with hydrochloric acid (1 M, 700 mL). The aqueous layer was extracted with dichloromethane (3 × 150 mL), washed with brine (200 mL), and dried over $MgSO_4 \cdot H_2O$, and the solvent was removed under vacuum. The product was obtained by purification via flash column chromatography.

*Synthesis of 1-Benzyl-5-(diphenylphosphino)-1H-tetrazole (**8**).* Under a nitrogen atmosphere, 1-benzyl-1*H*-tetrazole (3.12 mmol, 1.00 equiv) was dissolved in dry tetrahydrofuran (8 mL) and cooled to −100 °C, and *n*-butyllithium (2.5 M in *n*-hexane, 3.43 mmol, 1.10 equiv) was added dropwise via cannula. The reaction mixture was stirred at −100 °C for 30 min, and subsequently a solution of chlorodiphenylphosphane (3.43 mmol, 1.10 equiv) in dry tetrahydrofuran (2 mL) was added slowly via cannula. The reaction mixture was warmed to room temperature overnight. After quenching with water (3 mL), the mixture was filtered through a plug of silica gel. The product was obtained by purification via flash column chromatography.

*General Procedure for the Syntheses of Complexes **1-I**−**5-I**, **5-I(a)**, **6-I(a)**, and **8-I**.* Copper(I) iodide (0.40 mmol, 2.00 equiv) and the P^N ligand (0.60 mmol, 3.00 equiv) were suspended under nitrogen in dry dichloromethane (10 mL) and stirred for 12 h at room temperature, resulting in a clear solution. Afterward the complex was purified through precipitation with diethyl ether, pentane, methyl *tert*-butyl ether, or cyclohexane (100 mL). The solid was filtered off, washed with the appropriate solvent, and dried under vacuum.

*General Procedure for the Syntheses of Complexes **5-I(b)**−**7-I(b)**.* Copper(I) iodide (0.40 mmol, 1.00 equiv) and the P^N ligand (0.40 mmol, 1.00 equiv) were suspended under nitrogen in dry dichloromethane (10 mL) and stirred for 12 h at room temperature. The complexes were purified through repeated precipitation in diethyl ether or methyl *tert*-butyl ether (100 mL). The solid was filtered off, washed with diethyl ether, and dried under vacuum.

*[(5-(Diphenylphosphino)-1-propyl-1H-1,2,4-triazole)$_3$Cu$_2$I$_2$] (**1-I**).* Yield: 519 mg, 0.41 mmol, 81%; white powder. IR (ATR): $\tilde{\nu}$ 2965 (vw), 1481 (w), 1435 (w), 1272 (w), 1174 (w), 1096 (w), 1028 (w), 998 (w), 971 (vw), 742 (m), 692 (m), 671 (w), 509 (m), 473 (m) cm^{-1}. MS (FAB), m/z (%): 1224 (1), 1034 (21), 843 (35), 740 (21), 653 (43), 548 (79), 358 (94), 297 (100). Anal. Calcd for $C_{51}H_{54}Cu_2I_2N_9P_3$ (1266.9): C, 48.35; H, 4.30; N, 9.95. Found: C, 48.10; H, 4.27; N, 10.06.

*[(5-(Diphenylphosphino)-1-butyl-1H-1,2,4-triazole)$_3$Cu$_2$I$_2$] (**2-I**).* Yield: 220 mg, 0.17 mmol, 62%; white powder. IR (ATR): $\tilde{\nu}$ 2958 (vw), 2871 (vw), 1480 (w), 1434 (w), 1271 (w), 1174 (w), 1096 (w), 1044 (m), 998 (vw), 971 (vw), 876 (vw), 742 (m), 692 (m), 670 (w), 510 (m), 475 (w) cm^{-1}. MS (FAB), m/z (%): 1252 (3), 1062 (25), 871 (35), 754 (23), 681 (52), 562 (89), 372 (98), 310 (100). Anal.

dx.doi.org/10.1021/ic4019162 | Inorg. Chem. 2013, 52, 13509−13520

Calcd for $C_{54}H_{60}Cu_2I_2N_9P_3$ (1308.9): C, 49.55; H, 4.62; N, 9.63. Found: C, 49.44; H, 4.56; N, 9.58.

*[(5-(Diphenylphosphino)-1-hexyl-1H-1,2,4-triazole)$_3$Cu$_2$I$_2$] (**3-I**).* Yield: 506 mg, 0.36 mmol, 61%; white powder. IR (ATR): $\tilde{\nu}$ 2923 (vw), 2853 (vw), 1481 (w), 1435 (w), 1272 (w), 1175 (w), 1096 (w), 1050 (vw), 1027 (vw), 998 (vw), 971 (vw), 876 (vw), 741 (w), 691 (m), 508 (m), 466 (w) cm^{-1}. MS (FAB), *m*/*z* (%): 1308 (2), 1119 (15), 927 (18), 782 (18), 737 (44), 590 (75), 400 (100), 338 (90). Anal. Calcd for $C_{60}H_{72}Cu_2I_2N_9P_3$ (1393.1): C, 51.73; H, 5.21; N, 9.05. Found: C, 51.47; H, 5.09; N, 8.80.

*[(5-(Diphenylphosphino)-1-benzyl-1H-1,2,4-triazole)$_3$Cu$_2$I$_2$] (**4-I**).* Yield: 480 mg, 0.34 mmol, 88%; white powder. IR (ATR): $\tilde{\nu}$ 3050 (vw), 1481 (vw), 1435 (w), 1328 (vw), 1272 (w), 1173 (vw), 1097 (w), 1028 (vw), 999 (vw), 971 (vw), 743 (w), 719 (w), 691 (m), 669 (w), 584 (vw), 516 (m), 467 (w) cm^{-1}. MS (FAB), *m*/*z* (%): 1283 (2), 1130 (22), 940 (49), 749 (21), 595 (85), 405 (62), 343 (100). Anal. Calcd for $C_{63}H_{54}Cu_2I_2N_9P_3$ (1409.0): C, 53.63; H, 3.86; N, 8.93. Found: C, 53.25; H, 3.81; N, 8.73.

*[(2-(Diphenylphosphino)-5-phenyl-1,3,4-oxadiazole)$_3$Cu$_2$I$_2$] (**5-I(a)**).* Yield: 683 mg, 0.50 mmol, 78%; yellow powder. IR (ATR): $\tilde{\nu}$ 3051 (vw), 2921 (vw), 2847 (vw), 1550 (w), 1481 (w), 1435 (w), 1340 (vw), 1159 (vw), 1095 (w), 1068 (w), 1027 (vw), 990 (vw), 956 (vw), 925 (vw), 778 (vw), 742 (w), 688 (m), 526 (w), 510 (w) cm^{-1}. MS (FAB), *m*/*z* (%): 1242 (3), 1104 (3), 915 (17), 775 (5), 583 (31). Anal. Calcd for $C_{60}H_{45}Cu_2I_2N_6O_3P_3$ (1371.9): C, 52.53; H, 3.31; N, 6.13. Found: C, 52.64; H, 3.68; N, 5.73.

*[(2-(Diphenylphosphino)-5-phenyl-1,3,4-oxadiazole)$_4$Cu$_4$I$_4$] (**5-I(b)**).* Yield: 155 mg, 0.07 mmol, 25%; yellow powder. IR (ATR): $\tilde{\nu}$ 3053 (vw), 1551 (w), 1481 (w), 1435 (w), 1341 (vw), 1095 (w), 1068 (vw), 1027 (vw), 988 (vw), 956 (vw), 778 (vw), 742 (w), 688 (vw), 525 (w), 507 (w) cm^{-1}. MS (FAB), *m*/*z* (%): 1434 (21), 1244 (2), 1104 (43), 915 (18), 774 (61), 723 (25), 583 (51). Anal. Calcd for $C_{80}H_{60}Cu_4I_4N_8O_4P_4$ (2083.1): C, 46.13; H, 2.90; N, 5.38. Found: C, 46.08; H, 3.02; N, 5.10.

*[(2-(Diphenylphosphino)-5-(p-tolyl)-1,3,4-oxadiazole)$_3$Cu$_2$I$_2$] (**6-I(a)**).* Yield: 236 mg, 0.17 mmol, 29%; yellow powder. IR (ATR): $\tilde{\nu}$ 1613 (vw), 1582 (vw), 1554 (vw), 1495 (w), 1434 (w), 1333 (vw), 1182 (vw), 1095 (w), 1077 (w), 1021 (vw), 989 (vw), 955 (vw), 823 (w), 733 (w), 690 (w), 621 (w), 505 (m), 464 (w) cm^{-1}. MS (FAB), *m*/*z* (%): 1287 (2), 1133 (9), 943 (38), 789 (11), 751 (35), 597 (100), 407 (28), 345 (18). Anal. Calcd for $C_{63}H_{51}Cu_2I_2N_6O_3P_3$ (1413.9): C, 53.53; H, 3.64; N, 5.94. Found: C, 53.90; H, 3.68; N, 5.86.

*[(2-(Diphenylphosphino)-5-(p-tolyl)-1,3,4-oxadiazole)$_4$Cu$_4$I$_4$] (**6-I(b)**).* Yield: 763 mg, 0.36 mmol, 82%; yellow powder. IR (ATR): $\tilde{\nu}$ 1615 (w), 1556 (w), 1495 (m), 1481 (w), 1435 (w), 1097 (w), 1077 (w), 988 (w), 827 (w), 742 (m), 735 (m), 691 (m), 623 (w), 527 (m), 514 (m), 503 (m), 478 (w), 459 (w), 441 (w), 428 (w) cm^{-1}. MS (FAB), *m*/*z* (%): 1476 (25), 1287 (3), 1133 (25), 941 (10), 789 (32), 597 (22). Anal. Calcd for $C_{84}H_{68}Cu_4I_4N_8O_4P_4$ (2139.2): C, 47.16; H, 3.20; N, 5.24. Found: C, 47.35; H, 3.29; N, 5.21.

*[(2-(Diphenylphosphino)-5-phenyl-1,3,4-thiadiazole)$_4$Cu$_4$I$_4$] (**7-I(b)**).* Yield: 347 mg, 0.16 mmol, 84%; orange powder. IR (ATR): $\tilde{\nu}$ 1480 (w), 1456 (w), 1434 (w), 1425 (w), 1097 (w), 764 (w), 740 (m), 689 (m), 641 (w), 512 (m), 501 (m), 490 (m), 444 (w) cm^{-1}. MS (FAB), *m*/*z* (%): because of the insolubility of the compound, no mass spectra could be measured. Anal. Calcd for $C_{80}H_{60}Cu_4I_4N_8O_4P_4 \cdot {}^1/_4$MTBE (2147.3): C, 44.98; H, 2.93; N, 5.17; S, 5.91. Found: C, 45.38; H, 2.85; N, 5.02; S, 6.07.

*[(1-Benzyl-5-(diphenylphosphino)-1H-tetrazole)$_3$Cu$_2$I$_2$] (**8-I**).* Yield: 219 mg, 0.15 mmol, 18%; white powder. IR (ATR): $\tilde{\nu}$ 1482 (w), 1436 (w), 1184 (vw), 1159 (vw), 1099 (w), 1027 (vw), 999 (w), 781 (vw), 747 (m), 720 (m), 693 (s), 592 (w), 516 (m), 469 (m) cm^{-1}. MS (FAB), *m*/*z* (%): 1284 (2), 1132 (2), 942 (32), 786 (2), 751 (10), 599 (35), 379 (72). Anal. Calcd for $C_{60}H_{51}Cu_2I_2N_{12}P_3$ (1414.0): C, 50.97; H, 3.64; N, 11.89. Found: C, 50.81; H, 3.57; N, 11.68.

X-ray Crystallography. The crystal structure determinations of **2-I**, **3-I**, **5-I(b)**, **5-I(b)′**, **7-I(b)**, and **8a-I** were performed on a Bruker-Nonius APEXII diffractometer (**3-I**, **5-I(b)**, **5-I(b)′**, **7-I(b)**, **8a-I**) or a Bruker-Nonius KappaCCD diffractometer (**2-I**) at 123(2) K using Mo Kα radiation (λ = 0.71073 Å). Crystal data, data collection parameters, and results of the analyses are given in Table S1 (Supporting Information). Direct methods (for **7-I(b)** and **8a-I** Patterson methods) were used for structure solution (SHELXS-97), and refinement was carried out using SHELXL-97 (full-matrix least squares on F^2).[81] Hydrogen atoms were refined using a riding model. A semiempirical absorption correction using equivalent reflections was applied (see Table S1).

In **3-I** one phenyl group and one *n*-hexyl group are disordered (sof = 0.63(1) and 0.54(1), respectively). In **5-I(b)** (crystallographic C_i symmetry) one phenyl group (sof = 0.544(5)) and the solvent MTBE and water (over the center of symmetry, sof = 0.50) are disordered. The water hydrogen atoms could not be localized (due to the disorder) and were not included in the refinement. In **5-I(b)′** (crystallographic C_2 symmetry) the solvent Et_2O and water are disordered (over the 2-fold axis, sof = 0.50). The water hydrogen atoms could not be localized (due to the disorder) and were not included in the refinement. In **8-I** one phenyl group (sof = 0.66(1)) and the copper atoms are disordered (major and minor isomer in the ratio 95:5).

Photophysical Measurements. Steady-state emission spectra were recorded on a FluoroMax-4 spectrofluorometer from Horiba Scientific equipped with a 150 W xenon arc lamp, excitation and emission monochromators (1200 grooves/nm blazed at 330 nm (excitation) and 500 nm (emission)), and a Hamamatsu R928 photomultiplier tube. Emission and excitation spectra were corrected for source intensity (lamp and grating) by standard correction curves. Decay time measurements were recorded and detected on the same system using the TCSPC method with the FM-2013 accessory and a TDSPC hub from Horiba Yvon Jobin. A NanoLED 370 was used as excitation source (λ 371 nm, 1.5 ns pulse). The quality of the fit was assured by minimizing the χ^2 function and by visual inspection of the weighted residuals. Luminescence quantum yields were measured with a Hamamatsu Photonics absolute PL quantum yield measurement system (C9920-02G) equipped with a L9799-01 CW xenon light source (150 W), monochromator, C7473 photonic multichannel analyzer, and integrating sphere, and U6039-05 PLQY measurement software was used (Hamamatsu Photonics, Ltd., Shizuoka, Japan). All solvents used were of spectrometric grade. Degassed samples were prepared by purging with argon for 30 min. UV−vis absorption spectra were measured on a Thermo Scientific Evolution 201 UV−visible spectrophotometer.

Computational Methods. Density functional theory (DFT) calculations of complexes **2-I**, **5-I(b)**, and **7-I(b)** as well as ligands **1**−**8** were performed using BP86[82,83] and B3LYP[84,85] as functionals and the def2-SV(P) basis set.[86,87] For numerical integration, the m4 grid was employed. In the BP86 calculations the resolution of identity (RI) approximation was used.[88−90] The initial structures of the complexes were obtained from single-crystal X-ray diffraction data and were optimized using the BP86 functional. Triplet structures were optimized using unrestricted DFT. Analytical harmonic vibrational frequency calculations were performed to verify that the optimized complex structures are minima on the potential energy surface. Frontier orbitals depicted in Figures 6 and 10 were calculated using B3LYP at BP86 optimized geometries. All calculations were done using the Turbomole program package (version 6.4).[91]

RESULTS AND DISCUSSION

Synthesis and Structural Studies. The P^N ligands studied in this work are tetrazoles, 1,2,4-triazoles, oxadiazoles, and thiadiazoles (Chart 1). These ligands are accessible through one- or two-step reactions following processes known from the literature.

For 1,2,4-triazole-based ligands **1**−**4**, the introduction of an additional alkyl substituent at the 1-position was possible in a one-step reaction followed by the introduction of diphenylphosphine via deprotonation of the appropriate alkyl-

dx.doi.org/10.1021/ic4019162 | Inorg. Chem. 2013, 52, 13509−13520

Chart 1. Different P^N Ligands Investigated for Their Complexation Behavior

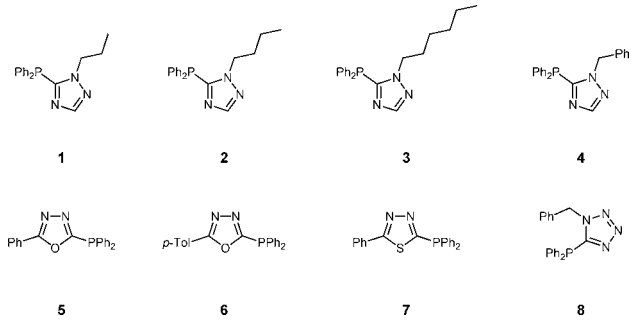

substituted triazole precursor with butyllithium and addition of chlorodiphenylphosphine. In the case of 1,2,4-triazoles, long alkyl groups were introduced in order to enhance the solubility of these compounds in nonpolar solvents such as chlorobenzene, toluene, xylene, and tetrahydrofuran.

Ligands with oxadiazole or thiadiazole moieties (**5**–**7**) can be synthesized by deprotonation of the appropriate heterocyclic precursors (**14**–**16**) with triethylamine followed by the addition of chlorodiphenylphosphine. Ligand **8** with a tetrazole moiety is accessible starting at benzylamine, which can be reacted with sodium azide and triethyl orthoformate to the benzyl-substituted tetrazole precursor. Deprotonation of this molecule at −100 °C followed by the addition of chlorodiphenylphosphine results in the target compound (Scheme 1).

These ligands were investigated with regard to their complexation abilities with copper(I). Copper(I) iodide was used as the metal salt due to its better oxidation stability in comparison to copper(I) bromide or copper(I) chloride. In addition, in the case of dinuclear complexes based on pyridylphosphine ligands, it has been shown that copper(I) iodide complexes feature better photoluminescence characteristics.[38] The complexes were synthesized by mixing the appropriate ligands with copper(I) iodide in different molar ratios. After they were stirred in dichloromethane at room temperature for several hours, the reaction mixtures cleared up, indicating the end of the reaction. Pure complexes were available after precipitation with diethyl ether, methyl *tert*-butyl ether, or hexane from the filtered reaction mixture and subsequent washing with the solvent used for precipitation. Single crystals were obtained by slow diffusion of diethyl ether or methyl *tert*-butyl ether into the reaction mixture or into a saturated dichloromethane solution of the corresponding complex. Complexes were characterized using mass spectroscopy, elemental analysis, and, where possible, single-crystal X-ray diffraction.

Scheme 1. Synthesis of P^N-type Ligands 1–8[a]

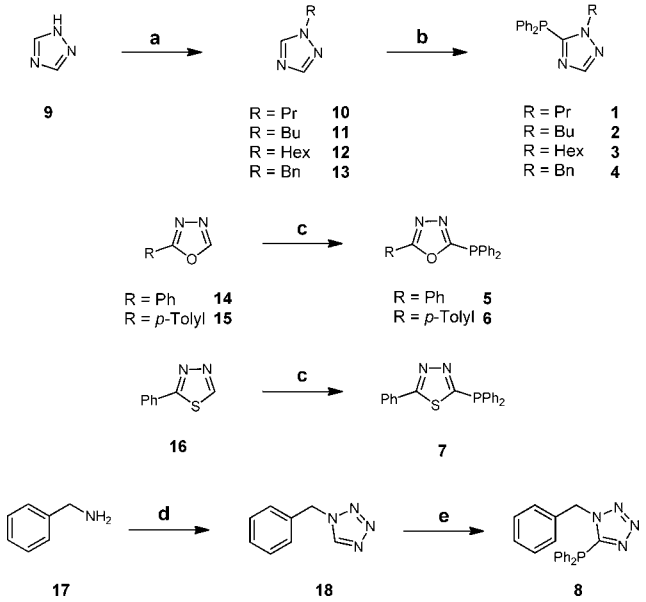

[a]Reagents and conditions: (a) DBU, R–X, THF, room temperature; (b) (1) *n*-BuLi, THF −78 °C, (2) Ph_2PCl, −78 °C to room temperature; (c) NEt_3, Ph_2PCl, pyridine, room temperature; (d) NaN_3, $HC(OEt)_3$, AcOH, 80 °C; (e) (1) *n*-BuLi, THF, −100 °C, (2) Ph_2PCl, −100 °C to room temperature.

X-ray structure analyses reveal three different complex structures using these five-membered heterocycles as coordinating P^N ligands: two dinuclear complexes with different structures and one tetranuclear complex structure. Complexes **1-I**–**4-I**, **5-I(a)**, and **6-I(a)** using 1,2,4-triazoles or oxadiazoles as bridging ligands were synthesized by reacting the appropriate P^N ligand together with copper(I) iodide in a 3:2 molar ratio. These compounds feature a dinuclear complex structure with a Cu_2I_2 metal halide core surrounded by three ligands (see Figure 1).

One ligand acts as a bridging unit, while the other two ligands coordinate only via their phosphorus atoms. Selected bond distances and angles are shown in Table S2 in the Supporting Information. This structural motif is also found for the corresponding complexes based on 2-pyridylphosphane ligands.[38] Changing the metal to ligand ratio from 3:2 to 1:1 results in the formation of tetranuclear complexes of $L_4Cu_4I_4$ stoichiometry in the case of ligands based on oxadiazoles (**5-I(b)** and **6-I(b)**), while ligands containing 1,2,4-triazoles still yield dinuclear complexes of $L_3Cu_2I_2$ stoichiometry. Because of structural similarities, thiadiazole **7** was used to synthesize the tetranuclear complex **7-I(b)** in order to investigate the effect of different electronic characteristics of the P^N ligands.

The structures of complexes **5-I(b)** and **7-I(b)** are shown in Figure 2; selected bond lengths and angles are given in Tables S3 and S4 in the Supporting Information.

The tetranuclear copper halide core can be seen as a dimer of Cu_2I_2 dimers, each showing a butterfly-shaped structure. The copper atoms of each subunit are coordinated by one bridging P^N ligand. Two other P^N ligands act as monodentate ligands coordinating one copper atom of each subunit via their phosphorus atoms. One of the bridging halide atoms in each Cu_2I_2 core coordinates a copper atom of the other subunit and thus links the two subunits. As mentioned before, ligand **6** behaves similarly to ligand **5** and forms the corresponding complexes **6-I(a)** and **6-I(b)**, depending on the exact molar ratio between P^N ligand and copper salt used for synthesizing the corresponding complex.

Another different structure of a dinuclear complex was obtained using 1-benzyl-5-(diphenylphosphino)-1*H*-tetrazole (**8**) as ligand. Again, the synthesis was carried out as described above and the obtained complex powder was analyzed via elemental analysis, confirming a structure with a 3:2 stoichiometry for complex **8-I**. However, single crystals were analyzed, revealing a dinuclear complex with different ligands as shown in Figure 3 (complex **8a-I**). Obviously, a rearrangement of the ligands according to Scheme 2 took place, which resulted

dx.doi.org/10.1021/ic4019162 | *Inorg. Chem.* 2013, 52, 13509–13520

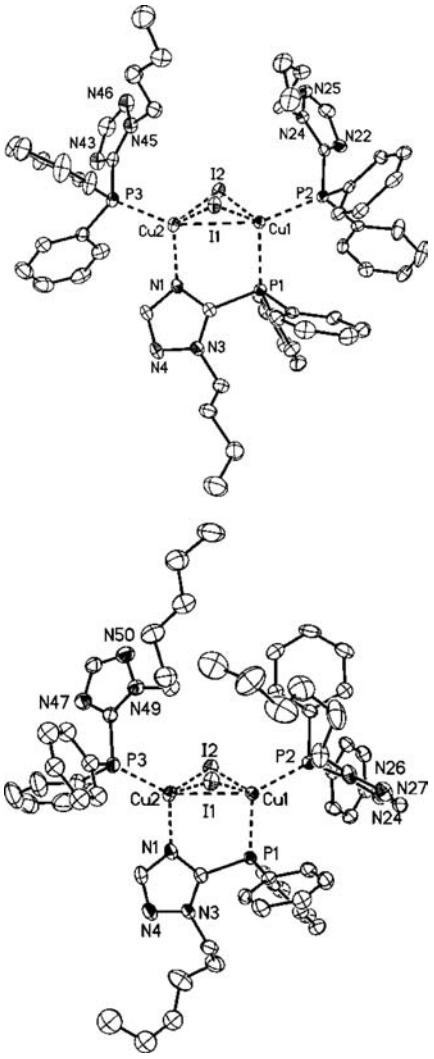

Figure 1. Molecular structure of complexes **2-I** (top) and **3-I** (bottom). Hydrogen atoms and minor disordered parts are omitted for clarity; displacement parameters are drawn at the 50% probability level.

in the transfer of a diphenylphosphino group from one ligand to the benzyl carbon atom of another ligand with substitution of a hydrogen atom. Tetrazoles are known for their wide range of rearrangement reactions, and keeping in mind that copper is a metal known for its multifaceted catalytical activities, a kind of copper-mediated rearrangement reaction seems to take place.[92−96] However, since this is a nontrivial task to clarify, detailed studies on the exact reaction mechanisms will be necessary and are currently in the focus of our research work.

As shown in Figure 3, ligand **8a** acts as chelating ligand via its two phosphorus atoms. Each copper atom is tetrahedrally coordinated by two iodides and two phosphines, and the resulting complex structure features a copper−copper distance of 3.16 Å (Table S5, Supporting Information).

Such a complex structure with a butterfly-shaped copper halide core and two chelating bisphosphines ligands is rare in the literature, but has been reported by Tsuboyama et al. with 1,2-bis(diphenylphosphino)benzene as chelating ligand.[42]

In summary, copper(I) complexes based on five-membered heterocycles exhibit a high structural diversity. Dinuclear complexes **1-I**−**4-I**, **5-I(a)**, and **6-I(a)** with the stoichiometry $L_3Cu_2I_2$ are obtained using ligands with 1,2,4-triazole or

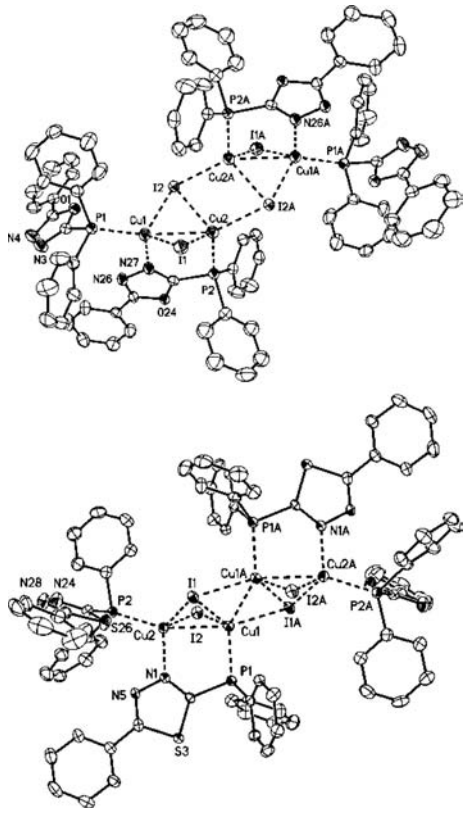

Figure 2. Molecular structure of complexes **5-I(b)** (top) and **7-I(b)** (bottom). Hydrogen atoms and minor disordered parts are omitted for clarity; displacement parameters are drawn at the 50% probability level.

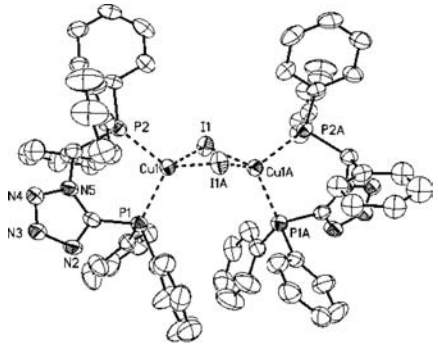

8a-I

Figure 3. Molecular complex structure of complex **8a-I**. Hydrogen atoms and minor disordered parts are omitted for clarity; displacement parameters are drawn at the 50% probability level.

Scheme 2. Structural Rearrangement in the Ligand Sphere of Complex 8-I Yielding Complex 8a-I

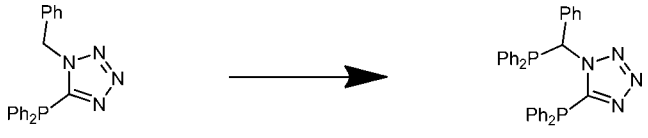

8 **8a**

oxadiazole moieties and a 3:2 molar ratio between P^N ligand and metal salt. Additionally tetranuclear complexes **5-I(b)**, **6-I(b)**, and **7-I(b)** of $L_4Cu_4I_4$ stoichiometry can be synthesized

dx.doi.org/10.1021/ic4019162 | *Inorg. Chem.* 2013, 52, 13509−13520

by reacting oxadiazole- or thiadiazole-containing P^N ligands in a 1:1 stoichiometry. Finally, by using 1-benzyl-5-(diphenylphosphino)-1*H*-tetrazole (**8**) as ligand, complex **8-I** of $L_3Cu_2I_2$ stoichiometry is accessible. However, a rearrangement in the ligand sphere leading to the dinuclear complex **8a-I** of stoichiometry $L_2Cu_2I_2$ took place, as revealed by single-crystal X-ray measurements. Investigations on the detailed reaction mechanism are ongoing. The results of the different aforementioned complexation reactions are also summarized in Table 1.

Table 1. Summary of the Syntheses of Different Copper(I) Complexes in This Study

ligand	complex	L:M[a]	stoichiometry[b]	structure[c]
1	**1-I**	3:2	$L_3Cu_2I_2$	
2	**2-I**	3:2	$L_3Cu_2I_2$	$L_3Cu_2I_2$
3	**3-I**	3:2	$L_3Cu_2I_2$	$L_3Cu_2I_2$
4	**4-I**	3:2	$L_3Cu_2I_2$	
5	**5-I(a)**	3:2	$L_3Cu_2I_2$	
5	**5-I(b)**	1:1	$L_4Cu_4I_4$	$L_4Cu_4I_4$[97]
6	**6-I(a)**	3:2	$L_3Cu_2I_2$	
6	**6-I(b)**	1:1	$L_4Cu_4I_4$	
7	**7-I(b)**	1:1	$L_4Cu_4I_4$[98]	$L_4Cu_4I_4$
8	**8-I**	3:2	$L_3Cu_2I_2$	$L_2Cu_2I_2$[d]

[a]Ligand-to-metal ratio used for the synthesis of the complex. [b]Based on elemental analysis of the isolated complex powder after precipitation and washing of the complex. [c]Result of single-crystal X-ray structure analysis if existent. [d]Due to rearrangement in the ligand sphere of the complex in solution.

Photophysical and Theoretical Characterization. Absorption spectra of complexes **1-I**, **4-I**, **5-I(a)**, and **5-I(b)** were measured in dichloromethane solution at room temperature.[99] These spectra are shown in Figure 4 along with those of the free ligands **4** and **5**. Spectra of **1** and **1-I** are omitted for clarity, since they are similar in shape to the spectra of **4** and **4-I**, but they are available in Figure S2 in the Supporting Information.

Dinuclear triazolylphosphane-based complexes **1-I** and **4-I** show a shoulder at 248 nm (ε = 43790 and 44630 M^{-1} cm^{-1}), which can be correlated to an absorption peak at 248 nm (ε = 13420 and 11830 M^{-1} cm^{-1}) in the free ligand spectra of **1** and **4**, respectively. These are assigned to $\pi-\pi^*$ transitions within the phenyl rings on the phosphane moieties. In addition, these complexes feature additional tails, which are not present in the corresponding free ligand spectra, ranging from 300 to 420 nm and from 300 to 380 nm (ε = 11990−9820 M^{-1} cm^{-1}) for complexes **1-I** and **4-I**, respectively. These low-energy bands are assigned to charge transfer transitions.

DFT calculations suggest that these transitions have metal to ligand charge transfer (MLCT) character mixed with halogen to ligand charge transfer (XLCT) character and are therefore assigned to (M+X)LCT states. The same trends can be observed in the spectra of **5**, **5-I(a)**, and **5-I(b)**, with peaks at 256, 261, and 262 nm (ε = 22632, 77510, and 107930 M^{-1} cm^{-1}, respectively) assigned to $\pi-\pi^*$ transitions within the phenyl rings on the phosphane moieties and additional tails at 320 nm to approximately 400 nm (ε = 6941−4322 M^{-1} cm^{-1}), which were assigned to (M+X)LCT transitions according to DFT calculations (see below). The absorption spectra of complexes **5-I(a)** and **5-I(b)** are very similar in shape and peak position. Keeping in mind that complex **5-I(a)** has a dinuclear structure and complex **5-I(b)** features a tetranuclear complex

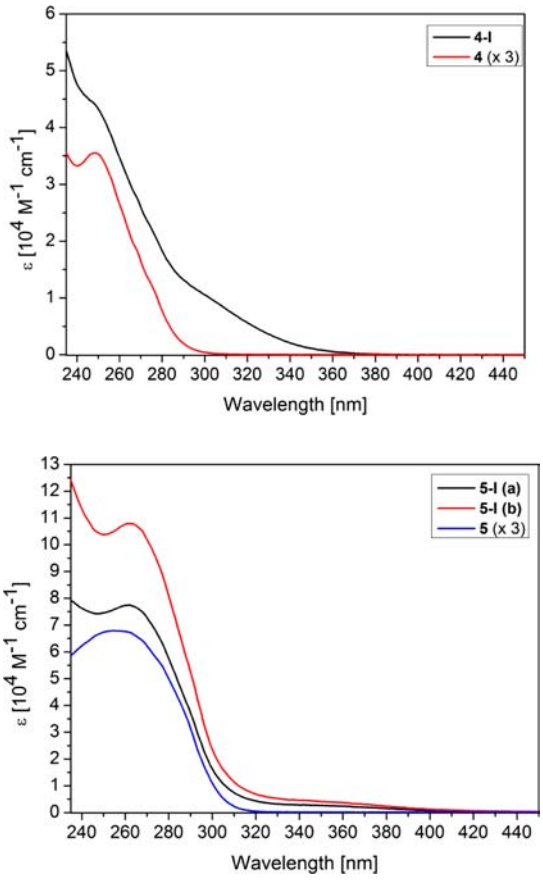

Figure 4. Absorption spectra of complexes **4-I**, **5-I(a)**, and **5-I(b)** as well as their corresponding ligands **4** and **5** at room temperature in dichloromethane solution.

structure, a possible explanation for the similarity would be that the photophysical properties of both complex structures are related to each other. This issue will be further discussed below on the basis of emission and lifetime measurements in solution.

The photophysical properties of neat complex powders of **1-I**−**4-I**, **5-I(a)**, **5-I(b)**, **6-I(a)**, **6-I(b)**, **7-I(b)**, and **8-I** were investigated. The emission spectra of complexes **2-I**, **3-I**, **5-I(a)**, **5-I(b)**, **6-I(b)**, **7-I(b)**, and **8-I** are displayed in Figures 5 and 9. In addition, the photophysical characteristics of all investigated complexes can be seen in Table 2. Emission spectra of complexes **1-I**, **4-I**, and **6-I(a)** are shown in Figure S3 in the Supporting Information for completeness, since they are similar in profile to the spectra shown in Figures 5 and 9.

The spectra of neat powder measurements of triazole complexes **1-I**−**4-I**, oxadiazole complexes **5-I(a)**, **5-I(b)**, **6-I(a)**, and **6-I(b)**, thiadiazole complex **7-I(b)**, and tetrazole complex **8-I** are broad and unstructured, indicating charge transfer processes, which is in agreement with the results gained from DFT calculations (see below). Complexes **1-I**−**4-I** with 1,2,4-triazole moieties exhibit luminescence maxima in the blue range of the visible spectrum at 485, 485, 458, and 496 nm (complexes **1-I**−**4-I**, respectively), while complexes **5-I(a)**, **6-I(a)**, and **8-I** with oxadiazole or tetrazole moieties have emission maxima in the green-yellow region at 544, 548, and 531 nm, respectively. All of these complexes have the same structure, namely $L_3Cu_2I_2$, and are therefore comparable with each other.

The assumption of (M+X)LCT transitions for the dinuclear complexes **1-I**−**4-I**, **5-I(a)**, **6-I(a)**, and **8-I** is in accordance with

dx.doi.org/10.1021/ic4019162 | *Inorg. Chem.* 2013, 52, 13509−13520

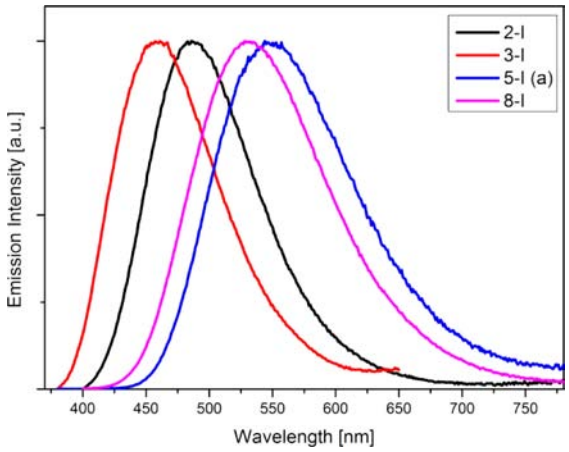

Figure 5. Neat powder measurements of complexes **2-I**, **3-I**, **5-I(a)**, and **8-I** (λ_{exc} 350 nm). For clarity, emission spectra of complexes **1-I**, **4-I**, and **6-I(a)** can be found in Figure S3 in the Supporting Information.

Table 2. Photoluminescence Characteristics[a]

compd	λ_{em} (nm)	Φ_{PL}[b]	τ_{av}[c] (μs)	k_r[d] (10^5 s^{-1})	k_{nr}[d] (10^5 s^{-1})
1-I	485	0.19	1.09	1.74	7.43
2-I	485	0.95	3.69	2.57	0.14
3-I	458	0.10	1.61	0.62	5.59
4-I	496	0.26	1.77	1.47	4.18
5-I(a)	544	0.70	1.81	3.87	1.66
5-I(b)	550	0.48	2.46	1.95	2.11
6-I(a)	548	0.68	1.19	5.71	2.69
6-I(b)	541	0.26	1.38	1.88	5.36
7-I(b)	617	0.45	1.27	3.54	4.33
8-I	531	0.47	1.05	4.48	5.05

[a]Neat powders at room temperature, λ_{exc} 350 nm. [b]Error ±5%. [c]Since the decay is best fitted by two or three exponentials, a weighted average lifetime (τ_{av}) is given, calculated by the equation $\tau_{av} = \sum A_i\tau_i / \sum A_i$, where A_i is the pre-exponential for the lifetime τ_i. The respective values can be seen in Table S6 in the Supporting Information. [d]Decay times at 512 and 549 nm, respectively.

the results gained from DFT calculations of **2-I**, showing that the HOMO resides on the copper iodide core and the LUMO is located in the ligand sphere (see Figure 6).

As can be seen from the data (Table 2), the emission maxima of the dinuclear complexes **1-I**–**4-I**, **5-I(a)**, **6-I(a)**, and **8-I** are red-shifted on going from triazole to tetrazole to oxadiazole moieties, indicating a decrease in the HOMO–LUMO gap. It has been previously reported that there is a correlation between ligand LUMO energy and the LUMO energy of complexes with

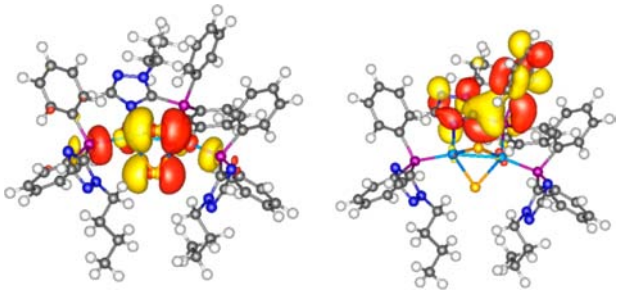

Figure 6. HOMO (left) and LUMO (right) of the dinuclear complex **2-I**.

identical structures featuring substituted pyridylphosphanes as P^N ligands: ligands with high LUMO energies lead to increasing LUMO energies of the resulting complexes.[38] The energy of the HOMO stays roughly the same, and thus a higher LUMO energy leads to a blue shift of the emission maximum.

Using the LUMO energy of the ligand to predict the emission wavelength is based on the assumption that there is not only a correlation between the complex LUMO and the ligand LUMO regardless of the complex structure but also a correlation of the complex LUMO and the emission energy, thus neglecting that the structural relaxation in the excited state might be different for different compounds. Considering the enormous structural variety of the complexes presented in this study, it is almost surprising that there is indeed a relationship between the energy of the ligand LUMO and the emission wavelength (see Figure 7).

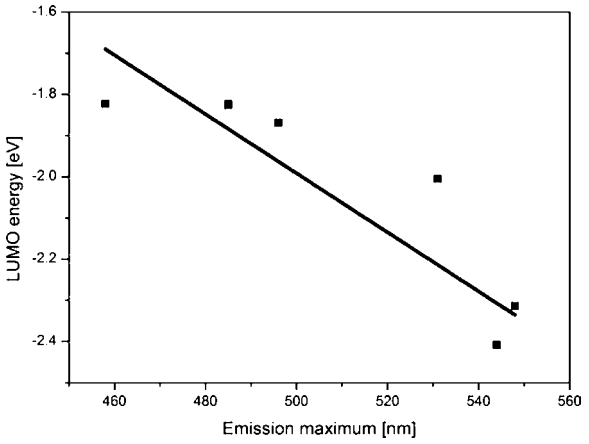

Figure 7. Correlation between ligand LUMO energies and emission maxima of the corresponding complexes (for exact values of the LUMO energies see Table S9 in the Supporting Information).

Measurements in dichloromethane solution, neat films, or PMMA matrices have been conducted in order to investigate the influence of different environments.[99] The emission spectra of complex **2-I** are shown in Figure 8 as a representative example for complexes with a 1,2,4-triazole moiety, while the emission spectra of complex **4-I** can be seen in Figure S4 in the

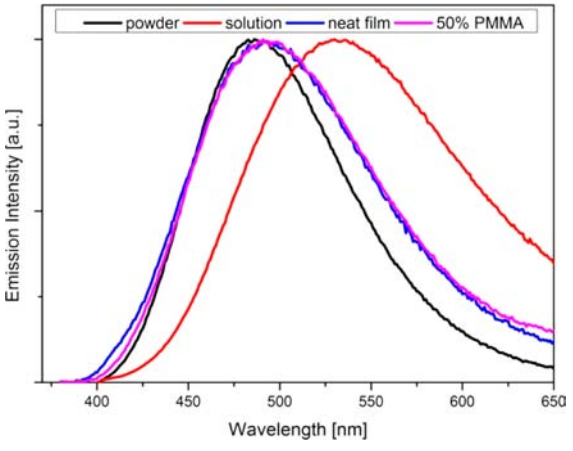

Figure 8. Photoluminescence spectra of complex **2-I** in different environments: powder, solution, neat film, and PMMA doped with 50% emitting compound (λ_{exc} 350 nm).

dx.doi.org/10.1021/ic4019162 | Inorg. Chem. 2013, 52, 13509–13520

Table 3. Luminescence Properties of Complexes 2-I and 4-I in Different Environments

	2-I					4-I				
complex	λ_{max} (nm)	Φ_{PL}[a]	τ_{av}[b] (μs)	k_r (10^5 s^{-1})	k_{nr} (10^5 s^{-1})	λ_{max} (nm)	Φ_{PL}[a]	τ_{av}[b] (μs)	k_r (10^5 s^{-1})	k_{nr} (10^5 s^{-1})
powder	486	0.95	3.69	2.57	0.14	495	0.26	1.77	1.47	4.18
neat film	492	0.42	1.40	3.00	4.14	495	0.43	1.62	2.65	3.52
50% PMMA	492	0.29	1.74	3.79	1.95	495	0.66	1.72	3.84	1.98
CH_2Cl_2 solution	532	0.03	0.10	3.00	9.70	541	0.03	0.21	1.42	46.2

[a]Error ±5%. [b]Since the decay is best fitted by using two or three exponentials, a weighted average lifetime (τ_{av}) is given, calculated by the equation $\tau_{av} = \sum A_i\tau_i/\sum A_i$, where A_i is the pre-exponential for the lifetime τ_i. The respective values can be seen in Table S7 in the Supporting Information.

Supporting Information. In Table 3, photophysical characteristics of these complexes are summarized. The emission maxima in dichloromethane solution are red-shifted in comparison to powder, film, or matrix measurements. This red shift is also present when comparing powder with film or matrix measurements, but it is less pronounced with the latter.

As can be seen from the data, complex **2-I** with a long alkyl substituent, i.e. a butyl group, exhibits a stronger red shift of the emission maxima in film or matrix measurements in comparison to that in powder measurements (as powder, 486 nm; as neat film or doped in PMMA, 492 nm; in CH_2Cl_2, 532 nm), while complex **4-I** with a benzyl substituent exhibits no red shift of the emission maxima in film or matrix measurements (as powder, 495 nm; as neat film or doped in PMMA, 495 nm; in CH_2Cl_2, 541 nm).

Emission quantum yields of all compounds as neat powders are shown in Table 2. The measured values for the dinuclear complexes are moderate to high, reaching values up to ϕ_{PL} = 0.95 for complex **2-I**, which is comparable to those found for dinuclear complexes based on pyridylphosphane ligands and other comparable copper(I) clusters.[38,42,67,101] The lower quantum yields for complexes **1-I**, **3-I**, and **4-I** might be explained by the influence of the different substituents, although the trend is not very clear.[38] Complex **1-I** and complex **3-I**, which have a shorter and a longer alkyl chain, respectively, show relatively small quantum yields with ϕ_{PL} = 0.19 and ϕ_{PL} = 0.10, and complex **4-I** with a benzyl substituent also features a rather small value of ϕ_{PL} = 0.26. Emission quantum yields of both complexes, **2-I** and **4-I**, as neat powders, films, or matrices are in the range of 29−66% but are significantly lower in dichloromethane solution at 3% (Table 3). Excited-state lifetimes of the dinuclear complexes are in the range 1.61−3.69 μs. The decay curves were best fitted with two- and three-exponential decays, which might be due to different structural environments, as was recently shown by the Coppens group.[100] They are comparable to the values found in similar complexes, dinuclear as well as tetranuclear in nature.[38,42,67,101] The exact values together with the corresponding radiative and nonradiative rate constants can be seen in Table 2.

Excited-state lifetimes of neat films or PMMA matrices doped with 50% of the emitting compound are in the range 1−2 μs for the investigated complexes **2-I** and **4-I** and are therefore slightly shorter than the values of neat complex powders. Emission decay times measured in dichloromethane solution are even shorter than those found in measurements of neat powders, films, or matrices with decay times of 0.1−0.3 μs. Simultaneously, the nonradiative rate constants increase up to $k_{nr} = 9.70 \times 10^{-5}$ and $k_{nr} = 46.2 \times 10^{-5}$, while the radiative rate constants remain roughly the same for powder, film, matrix, and solution measurements (Table 3). This behavior, i.e. the red shift of the emission maxima, the decrease of lifetimes and quantum yields, and the increase of the nonradiative rate constants, can be explained by molecular distortions in the excited state, which can occur more easily in less rigid environments such as solutions in comparison to environments of higher rigidity such as crystal powders, films, and matrices.[102] The emission maxima of tetranuclear complexes **5-I(b)**, **6-I(b)**, and **7-I(b)** are at 550, 541, and 617 nm, respectively. There seems to be a slight influence of the additional methyl group in ligand **5** in comparison to ligand **6**, leading to a marginal blue shift in the emission maxima of **6-I(b)** in comparison to **5-I(b)**. A clearly visible red shift is observed in the case of **7-I(b)** in comparison to **5-I(b)** or **6-I(b)**, as can be seen in Figure 9.

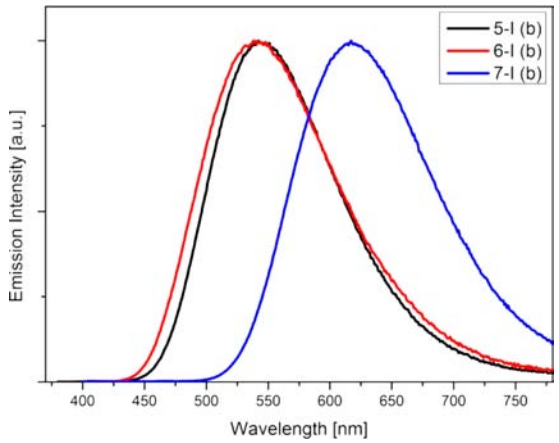

Figure 9. Neat powder measurements of complexes **5-I(b)**, **6-I(b)**, and **7-I(b)** (λ_{exc} 350 nm).

Dinuclear complexes **5-I(a)** and **6-I(a)** exhibit emission quantum yields with ϕ_{PL} = 0.70 and 0.68. Tetranuclear copper(I) complexes feature only slightly smaller quantum yields in comparison to their dinuclear counterparts, with values of ϕ_{PL} = 0.48, 0.26, and 0.45 for **5-I(b)**, **6-I(b)**, and **7-I(b)**. The emission decay times of the tetranuclear complexes are between 1.27 and 2.46 μs.

Complexes **5-I(b)** and **7-I(b)** were investigated using DFT. According to single-crystal diffraction data the complexes **5-I(b)** and **7-I(b)** have very similar structures. Because of the disorder in **5-I(b)**, the crystal structure of **7-I(b)** was used as the starting structure for the geometry optimization of both compounds and sulfur was substituted by oxygen to get complex **5-I(b)**. Single-crystal diffraction data show that these tetranuclear complexes can be regarded as dimers of two dinuclear complexes: both subunits contain a butterfly-shaped Cu_2I_2 core, a bridging P^N ligand, and one monodentate ligand. In addition, photophysical measurements of the dinuclear complexes **5-I(a)** and **6-I(a)** show emission maxima which differ only slightly from those of tetranuclear complexes **5-I(b)**

dx.doi.org/10.1021/ic4019162 | Inorg. Chem. 2013, 52, 13509−13520

and **6-I(b)** with values of 544 and 548 nm in comparison to 550 and 541 nm, respectively. This suggests that the dinuclear and the tetranuclear forms have similar electronic properties. The DFT calculations reveal that the HOMO resides on the Cu_4I_4 core and the LUMO on both bridging ligands (see Figure 10), similar to the frontier orbitals of the dinuclear complexes.

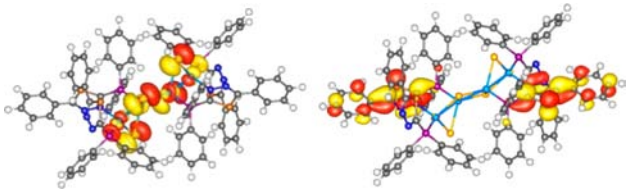

Figure 10. HOMO (left) and LUMO (right) of **7-I**.

Thus, an excitation from the HOMO to the LUMO has pronounced M+X to L charge transfer character. The phosphorescence energy of **7-I(b)**, which contains a thiadiazole ligand, is much smaller than the phosphorescence energy of **5-I(b)** with its oxadiazole ligand. The absolute values (0.96 eV for complex **7-I(b)** and 1.27 eV for complex **5-I(b)**) calculated as the energy difference between the lowest triplet state and the singlet ground state at the optimized triplet geometry, are red shifted by approximately 1 eV due to the insufficient description of charge transfer excitations using BP86. Despite the large red shift, the difference between the phosphorescence of **5-I(b)** and **7-I(b)** is calculated to be 0.3 eV, which agrees very well with measured emission energies of 2.25 and 2.01 eV, respectively.

The photophysical properties of the dinuclear complex **5-I(a)** and the tetranuclear complex **5-I(b)** were investigated additionally in dichloromethane solution, and the spectra are shown in Figure 11 along with the powder spectra. The

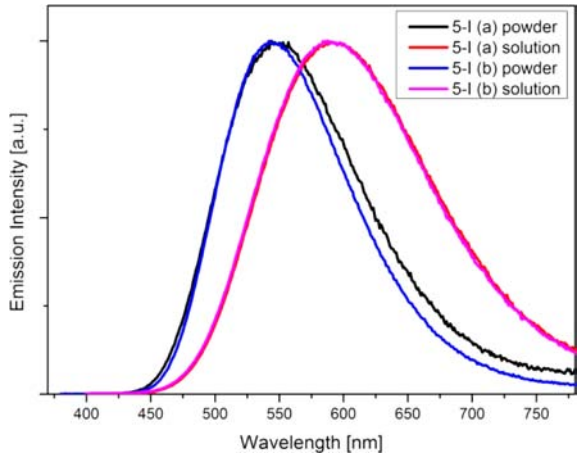

Figure 11. Measurement of complexes **5-I(a)** and **5-I(b)** as neat powders and in dichloromethane solution (λ_{exc} 350 nm).

emission maxima of neat powder measurements of both complexes (544 and 550 nm) are very similar, and the emission maxima in solution (589 and 588 nm) are almost identical, where the latter are red-shifted in comparison to the powder measurements. The similarity of the emissions suggests that both complex structures have similar electronic properties responsible for their photophysical charactertistics, as was also seen in DFT calculations. Lifetime measurements support this hypothesis, since they are similar: 0.52 μs for **5-I(a)** and 0.64 μs for **5-I(b)**.

Low-temperature measurements have been performed for complexes **1-I**–**4-I**, **5-I(a)**, **5-I(b)**, **7-I(b)**, and **8-I**. Figure 12

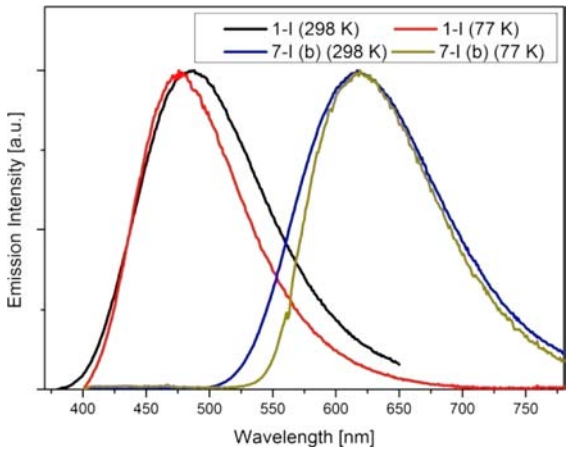

Figure 12. Emission spectra of neat complex powders of complexes **1-I** and **7-I(b)** at ambient temperature and at 77 K (λ_{exc} 350 nm).

shows luminescence spectra of representative examples for dinuclear and tetranuclear complexes **1-I** and **7-I(b)** measured as neat powders at 77 K and at room temperature. The corresponding spectra of complexes **2-I**–**4-I**, **5-I(a)**, **5-I(b)**, and **8-I** are similar in shape and are therefore omitted for clarity, but they are available in Figures S5–S10 in the Supporting Information. The emission maxima of the investigated complexes **1-I**–**4-I**, **5-I(a)**, **5-I(b)**, **7-I(b)**, and **8-I** display a blue shift in the range 0–17 nm in comparison to the corresponding ambient-temperature spectra (Table 4).

Table 4. Photoluminescence Characteristics[a]

	λ_{em} (nm)		τ_{av}[b] (μs)	
complex	298 K	77 K	298 K	77 K
1-I	485	475	1.09	38.7
2-I	485	485	3.69	49.8
3-I	458	441	1.61	18.4
4-I	496	487	1.77	33.8
5-I(a)	544	539	1.81	24.8
5-I(b)	550	538	2.46	30.8
7-I(b)	617	617	1.27	62.3
8-I	531	525	1.05	40.9

[a]Neat powders at room temperature, λ_{exc} 350 nm. [b]Since the decay is best fitted by two exponentials, a weighted average lifetime (τ_{av}) is given, calculated by the equation $\tau_{av} = \sum A_i\tau_i / \sum A_i$, where A_i is the pre-exponential for the lifetime τ_i. The respective values can be seen in Table S8 in the Supporting Information.

In addition, excited-state lifetimes increase by an order of magnitude into the range of 24.8–62.3 μs, which can be explained by the suppression of thermally activated non-radiative processes at low temperature.[38] The observed blue shift of the emission maxima for complexes **1-I**–**4-I** is in contrast with the reported results of red-shifted emission maxima for dinuclear complexes of comparable structure, which were explained by an emission from a lower lying triplet state.[38,42,67] Blue-shifted emission maxima were found, for example, in Ir(III) or Re(I) complexes at low temperatures and

dx.doi.org/10.1021/ic4019162 | Inorg. Chem. 2013, 52, 13509–13520

are explained by the occurrence of rigidochromic effects.[103−105] A progressive blue shift can be observed for the complexes studied in this work by changing the environment from nonrigid media such as solvents to rigid media such as crystal powders at room temperature. This can be explained by rigidochromic effects, and a further blue shift at low temperature might be related to similar effects.

It may be possible that the emitting state in these complexes is less stabilized due to a more rigid environment at 77 K, resulting in a blue shift of the emission maxima at low temperature. It should be noted that the assignment of the exact nature of the emitting state, i.e. ^{1}MLCT or ^{3}MLCT, is a nontrivial task. Luminescent copper(I) complexes often show relatively short lifetimes at ambient temperature and red-shifted emission maxima along with significantly longer lifetimes at low temperature. Such a behavior can be attributed to a process called thermally activated delayed fluorescence.[56,106,107] According to this model, the emission of these complexes is assigned to ^{1}MLCT transitions at room temperature and to lower lying ^{3}MLCT transitions at low temperature. Therefore, a red shift of the emission maxima is observed.[38,56] The complexes studied in this work show that two effects might be present at low temperature: a blue shift due to rigidochromic effects and a red shift due to emission from lower lying triplet states. Obviously, a potential red shift is overcompensated by rigidochromic effects, resulting in a blue shift of the emission maxima.

CONCLUSION

Bridging P^N ligands bearing five-membered heterocyclic moieties have been investigated with regard to their complexation behavior with copper(I) iodide as the metal salt and with respect to the photophysical properties of the resulting complexes. Different structures were found, depending either on the nature of the ligand itself or on the ligand to metal ratios used for the complexation reaction. A dinuclear complex of the general composition $L_3Cu_2I_2$ was found for 1,2,4-triazole-based (complexes **1-I**−**4-I**) and oxadiazole-based (complexes **5-I(a)** and **6-I(a)**) P^N ligands, leading to a complex structure in which one ligand acts as a bridging ligand for the dinuclear, butterfly-shaped metal iodide core, while the other two ligands coordinate solely via their phosphorus atoms. In addition, in the case of oxadiazoles, a tetranuclear complex structure of the general composition $L_4Cu_4I_4$ was found by reacting the P^N ligand and the metal salt in a 1:1 molar ratio instead of a ratio of 3:2, leading to a new kind of complex structure.This structure can be regarded as a dimer of two dinuclear complexes: both subunits contain a butterfly-shaped Cu_2I_2 core, a bridging P^N ligand, and one monodentate ligand. Furthermore, it was possible to synthesize either the dinuclear or the tetranuclear complex by controlling the stoichiometry of ligand to metal salt. In the case of thiadiazoles, only the tetranuclear form was obtainable. Two different dinuclear complex structures showing a composition of $L_2Cu_2I_2$ were obtained by using a tetrazole ligand. In the case of the tetrazole complex, elemental analysis confirmed the presence of a dinuclear complex with $L_3Cu_2I_2$ stoichiometry. However, single-crystal X-ray analysis revealed a rearrangement in the ligand sphere of the complex, leading to a complex of $L_2Cu_2I_2$ stoichiometry. The exact reaction mechanism is currently under investigation.

The luminescence maxima of the dinuclear 1,2,4-triazole-based complexes are seen in the deep blue region of the visible spectrum in the range 458−496 nm, with quantum yields reaching values up to 95%. The dinuclear and tetranuclear complexes based on oxadiazole ligands show similar emission spectra measured as powders as well as in dichloromethane solution because both complexes have similar electronic properties. This is supported by DFT calculations, which reveal that the HOMO resides on the Cu_4I_4 core and the LUMO on both bridging ligands, similar to the frontier orbitals of the dinuclear complexes.

Low-temperature measurements at 77 K of both the dinuclear and the tetranuclear complexes revealed a blue shift of the emission maxima in comparison to the corresponding measurements at ambient temperature. This behavior was ascribed to rigidochromic effects, which were clearly visible while going from less rigid (i.e., dichloromethane solution) to more rigid (i.e., crystal powder) environments. In an even more rigid environment at 77 K the emitting state in these complexes might be less stabilized, which might lead to a further blue shift of the emission maxima.

In summary, P^N ligands based on five-membered heterocycles are an intriguing class of ligands, leading to several different complex structures with interesting photophysical properties. In particular, dinuclear complexes with a 1,2,4-triazole moiety exhibit emission maxima in the deep blue region (458−496 nm) together with high quantum yields up to 95% and are therefore well suited for potential applications as blue-emitting materials in organic light-emitting devices.

ASSOCIATED CONTENT

Supporting Information

CIF files, text, tables, and figures giving crystallographic data for **2-I**, **3-I**, **5-I(b)**, **5-I(b)′**, **7-I(b)**, and **8a-I**, spectroscopic data of compounds **2**, **3**, **7**, and **8**, additional photophysical spectra, and Cartesian coordinates (in Å) of the optimized BP86/def2-SV(P) ground-state and triplet geometries of compounds **2-I** and **7-I(b)**. This material is available free of charge via the Internet at http://pubs.acs.org. Crystallographic data have also been deposited with the Cambridge Crystallographic Database with the following deposition numbers: CCDC-913209 (**2-I**), CCDC-913210 (**3-I**), CCDC-913511 (**5-I(b)**), CCDC-913212 (**5-I(b)′**), CCDC-913213 (**7-I(b)**), and CCDC-913215 (**8a-I**).

AUTHOR INFORMATION

Corresponding Authors

*T.B.: e-mail, baumann@cynora.com.

*S.B.: fax, (+ 49) 721 608 48581; e-mail, braese@kit.edu.

Notes

The authors declare no competing financial interest.

ACKNOWLEDGMENTS

We acknowledge financial support from the KIT. We also thank the Deutsche Forschungsgemeinschaft (DFG) for support through project B2 of SFB/TRR 88and the German Federal Ministry of Education and Research (BMBF) in the funding program cyCESH.

REFERENCES

(1) Hoppe, H.; Sariciftci, N. S. *J. Mater. Res.* **2011**, *19*, 1924−1945.
(2) Schlenker, C. W.; Thompson, M. E. *Chem. Commun.* **2011**, *47*, 3702−3716.
(3) Clarke, T. M.; Durrant, J. R. *Chem. Rev.* **2010**, *110*, 6736−6767.
(4) Zhang, F.; Xu, X.; Tang, W.; Zhang, J.; Zhuo, Z.; Wang, J.; Wang, J.; Xu, Z.; Wang, Y. *Sol. Energy Mater. Sol. Cells* **2011**, *95*, 1785−1799.

(5) Segura, J. L.; Martin, N.; Guldi, D. M. *Chem. Soc. Rev.* **2005**, *34*, 31−47.
(6) Brédas, J.-L.; Norton, J. E.; Cornil, J.; Coropceanu, V. *Acc. Chem. Res.* **2009**, *42*, 1691−1699.
(7) You, Y.; Park, S. O. *Dalton Trans.* **2009**, 1267−1282.
(8) Mitschke, U.; Bäuerle, P. *J. Mater. Chem.* **2000**, *10*, 1471−1507.
(9) So, F.; Kido, J.; Burrows, P. *MRS Bull.* **2008**, *33*, 663−669.
(10) *Highly Efficient OLEDs with Phosphorescent Materials*; Yersin, H., Ed.; Wiley-VCH: Weinheim, Germany, 2008.
(11) Loo, Y.-L.; McCulloch, J. *MRS Bull.* **2008**, *33*, 653−662.
(12) Chi, Y.; Chou, P.-T. *Chem. Soc. Rev.* **2010**, *39*, 638−655.
(13) He, L.; Qiao, J.; Duan, L.; Dong, G.; Zhang, D.; Wang, L.; Qiu, Y. *Adv. Funct. Mater.* **2009**, *19*, 2950−2960.
(14) Tsuzuki, T.; Tokito, S. *Adv. Mater.* **2007**, *19*, 276−280.
(15) Yang, C.-H.; Cheng, Y.-M.; Chi, Y.; Hsu, C.-J.; Fang, F.-C.; Wong, K.-T.; Chou, P.-T.; Chang, C.-H.; Tsai, M.-H.; Wu, C.-C. *Angew. Chem., Int. Ed.* **2007**, *46*, 2418−2421.
(16) Lowry, M. S.; Bernhard, S. *Chem. Eur. J.* **2006**, *12*, 7970−7977.
(17) Ulbricht, C.; Beyer, B.; Friebe, C.; Winter, A.; Schubert, U. S. *Adv. Mater.* **2009**, *21*, 4418−4441.
(18) Lamansky, S.; Djurovich, P. I.; Murphy, D.; Abdel-Razzaq, F.; Kwong, R.; Tsyba, I.; Bortz, M.; Mui, B.; Bau, R.; Thompson, M. E. *Inorg. Chem.* **2001**, *40*, 1704−1707.
(19) Flamigni, L.; Barbieri, A.; Sabatini, C.; Ventura, B.; Barigelletti, F. *Top. Curr. Chem.* **2007**, *281*, 143−203.
(20) Yersin, H.; Rausch, A. F.; Czerwieniec, R. In *Physics of Organic Semiconductors*; Bruetting, W., Adachi, C., Holmes, R. J., Eds.; Wiley-VCH: Weinheim, Germany, 2012; p 371.
(21) Hofbeck, T.; Yersin, H. *Inorg. Chem.* **2010**, *49*, 9290−9299.
(22) Zhou, G.-J.; Wang, X.-Z.; Wong, W.-Y.; Yu, X.-M.; Kwok, H.-S.; Lin, Z. *J. Organomet. Chem.* **2007**, *692*, 3461−3473.
(23) Wong, W.-Y.; He, Z.; So, S.-K.; Tong, K.-L.; Lin, Z. *Organometallics* **2005**, *24*, 4079−4082.
(24) Che, C.-M.; Kwok, C.-C.; Lai, S.-W.; Rausch, A., F.; Finkenzeller, W., J.; Zhu, N.; Yersin, H. *Chem. Eur. J.* **2010**, *16*, 233−247.
(25) Rausch, A., F.; Murphy, L.; Williams, J. A. G.; Yersin, H. *Inorg. Chem.* **2012**, *51*, 312−319.
(26) Williams, J. A. G. *Top. Curr. Chem.* **2007**, *281*, 205−268.
(27) Williams, J. A. G.; Develay, S.; Rochester, D. L.; Murphy, L. *Coord. Chem. Rev.* **2008**, *252*, 2596−2611.
(28) Kalinowski, J.; Fattori, V.; Cocchi, M.; Williams, J. A. G. *Coord. Chem. Rev.* **2011**, *255*, 2401−2425.
(29) Kim, J. H.; Liu, M. S.; Jen, A. K.-Y.; Carlson, B.; Dalton, L. R.; Shu, C.-F.; Dodda, R. *Appl. Phys. Lett.* **2003**, *83*, 776−778.
(30) bLu, J.; Tao, Y.; Chi, Y.; Tung, Y. *Synth. Met.* **2005**, *155*, 56−62.
(31) Chou, P.-T.; Chi, Y. *Eur. J. Inorg. Chem.* **2006**, 3319−3332.
(32) Breu, J.; Kratzer, C.; Yersin, H. *J. Am. Chem. Soc.* **2000**, *122*, 2548−2555.
(33) Barbieri, A.; Accorsi, G.; Armaroli, N. *Chem. Commun.* **2008**, *19*, 2185−2193.
(34) Hsu, C.-W.; Lin, C.-C.; Chung, M.-W.; Chi, Y.; Lee, G.-H.; Chou, P.-T.; Chang, C.-H.; Chen, P.-Y. *J. Am. Chem. Soc.* **2011**, *133*, 12085−12099.
(35) Czerwieniec, R.; Hofbeck, T.; Crespo, O.; Laguna, A. M.; Gimeno, M. C.; Yersin, H. *Inorg. Chem.* **2010**, *49*, 3764−3767.
(36) Barakat, K. A.; Cundari, T. R.; M, A. *J. Am. Chem. Soc.* **2003**, *125*, 14228−14229.
(37) Igawa, S.; Hashimoto, M.; Kawata, I.; Hoshino, M.; Osawa, M. *Inorg. Chem.* **2012**, *51*, 5805−5813.
(38) Zink, D. M.; Bächle, M.; Baumann, T.; Nieger, M.; Kühn, M.; Wang, C.; Klopper, W.; Monkowius, U.; Hofbeck, T.; Yersin, H.; Bräse, S. *Inorg. Chem.* **2013**, *52*, 2292−2305.
(39) Zink, D. M.; Baumann, T.; Nieger, M.; Barnes, E. C.; Klopper, W.; Bräse, S. *Organometallics* **2011**, *30*, 3275−3283.
(40) Zhang, L.; Li, B.; Su, Z. *J. Phys. Chem. C* **2009**, *113*, 13968−13973.
(41) Che, G.; Su, Z.; Li, W.; Chu, B.; Li, M.; Hu, Z.; Zhang, Z. *Appl. Phys. Lett.* **2006**, *89*, 103511/1−103511/3.
(42) Tsuboyama, A.; Kuge, K.; Furugori, M.; Okada, S.; Hoshino, M.; Ueno, K. *Inorg. Chem.* **2007**, *46*, 1992−2001.
(43) Manbeck, G. F.; Brennessel, W. W.; Eisenberg, R. *Inorg. Chem.* **2011**, *50*, 3431−3441.
(44) McMillin, D. R.; Buckner, M. T.; Ahn, B. T. *Inorg. Chem.* **1977**, *16*, 943−945.
(45) Buckner, M. T.; McMillin, D. R. *J. Chem. Soc., Chem. Commun.* **1978**, 759−761.
(46) Blaskie, M. W.; McMillin, D. R. *Inorg. Chem.* **1980**, *19*, 3519−3522.
(47) McMillin, D. R.; Kirchhoff, J. R.; Goodwin, K. V. *Coord. Chem. Rev.* **1985**, *64*, 83−92.
(48) Harvey, P. D.; Knorr, M. *Macromol. Rapid Commun.* **2010**, *31*, 808−826.
(49) Peng, R.; Li, M.; Li, D. *Coord. Chem. Rev.* **2010**, *254*, 1−18.
(50) McMillin, D. R.; McNett, K. M. *Chem. Rev.* **1998**, *98*, 1201−1219.
(51) Crane, D. R.; DiBenedetto, J.; Palmer, C. E. A.; McMillin, D. R.; Ford, P. C. *Inorg. Chem.* **1988**, *27*, 3698−3700.
(52) Simon, J. A.; Palke, W. E.; Ford, P. C. *Inorg. Chem.* **1996**, *35*, 6413−6421.
(53) Crestani, M. G.; Manbeck, G. F.; Brennessel, W. W.; McCormick, T. M.; Eisenberg, R. *Inorg. Chem.* **2011**, *50*, 7172−7188.
(54) Ford, P. C.; Cariati, E.; Bourassa, J. *Chem. Rev.* **1999**, *99*, 3625−3647 and references therein.
(55) Hashimoto, M.; Igawa, S.; Yashima, M.; Kawata, I.; Hoshino, M.; Osawa, M. *J. Am. Chem. Soc.* **2011**, *133*, 10348−10351.
(56) Czerwieniec, R.; Yu, J.; Yersin, H. *Inorg. Chem.* **2011**, *50*, 8293−8301.
(57) Czerwieniec, R.; Yu, J.; Yersin, H. *Inorg. Chem.* **2012**, *51*, 1975.
(58) Yersin, H.; Czerwieniec, R.; Hupfer, A. *Proc. SPIE* **2012**, *8435*, 843508.
(59) Yersin, H.; Rausch, A. F.; Czerwieniec, R.; Hofbeck, T.; Fischer, T. *Coord. Chem. Rev.* **2011**, *255*, 2622−2652.
(60) Bergmann, L.; Friedrichs, J.; Mydlack, M.; Baumann, T.; Nieger, M.; Bräse, S. *Chem. Commun.* **2013**, *49*, 6501−6503.
(61) Kyle, K. R.; Ryu, C. K.; DiBenedetto, J. A.; Ford, P. C. *J. Am. Chem. Soc.* **1991**, *113*, 2954−2965.
(62) Fitchett, C. M.; Steel, P. J. *Inorg. Chem. Commun.* **2007**, *10*, 1297−1300.
(63) Schramm, V.; Pierre, A.; Hiller, W. *Acta Crystallogr.* **1984**, *C40*, 1840−1841.
(64) Hiller, W. *Acta Crystallogr.* **1986**, *C42*, 149−150.
(65) Engelhardt, L. M.; Healy, P. C.; Kildea, J. D.; White, A. H. *Aust. J. Chem.* **1989**, *42*, 913−922.
(66) Maeyer, J. T.; Johnson, T. J.; Smith, A. K.; Borne, B. D.; Pike, R. D.; Pennington, W. T.; Krawiec, M.; Rheingold, A. L. *Polyhedron* **2003**, *22*, 419−431.
(67) Araki, H.; Tsuge, K.; Sasaki, Y.; Ishizaka, S.; Kitamura, N. *Inorg. Chem.* **2005**, *44*, 9667−9675.
(68) Hirtenlehner, C.; Monkowius, U. *Inorg. Chem. Commun.* **2012**, *15*, 109−112.
(69) Eisler, D. J.; Kirby, C. W.; Puddephatt, R. J. *Inorg. Chem.* **2003**, *42*, 7626−7634 and references therein.
(70) Ahuja, R.; Nethaji, M.; Samuelson, A. G. *J. Organomet. Chem.* **2009**, *694*, 1144−1152.
(71) Ahuja, R.; Nethaji, M.; Samuelson, A. G. *Inorg. Chim. Acta* **2011**, *372*, 220−226.
(72) Maini, L.; Braga, D.; Mazzeo, P.; Ventura, B. *Dalton Trans.* **2012**, *41*, 531−539.
(73) Krylova, V. a; Djurovich, P. I.; Whited, M. T.; Thompson, M. E. *Chem. Commun.* **2010**, *46*, 6696−6698.
(74) Manbeck, G. F.; Brennessel, W. W.; Evans, C. M.; Eisenberg, R. *Inorg. Chem.* **2010**, *49*, 2834−2843.
(75) Breitmaier, E.; Jung, G. *Organic Chemistry*; Thieme: Stuttgart, Germany, 2001.
(76) Tolmachev, A. A.; Zarudnitskii, E. V.; Yurchenko, A. A.; Pinchuk, A. M. *Chem. Heterocycl. Compd.* **1999**, *35*, 1117−1119.

(77) Kawano, T.; Hirano, K.; Satoh, T.; Miura, M. *J. Am. Chem. Soc.* **2010**, *132*, 6900−6901.
(78) Gierczyk, B.; Zalas, M. *Org. Prep. Proced. Int.* **2005**, *37*, 213−222.
(79) Vorobiov, A. N.; Gaponik, P. N.; Petrov, P. T.; Ivashkevich, O. A. *Synthesis* **2006**, *8*, 1307−1312.
(80) Bulger, P. G.; Cottrell, I. F.; Cowden, C. J.; Davies, A. J.; Dolling, U.-H. *Tetrahedron Lett.* **2000**, *41*, 1297−1301.
(81) Sheldrick, G. M. *Acta Crystallogr.* **2008**, *A64*, 112−122.
(82) Becke, A. D. *Phys. Rev. A* **1988**, *38*, 3098−3100.
(83) Perdew, J. P. *Phys. Rev. B* **1986**, *33*, 8822−8827.
(84) Lee, C.; Yang, W.; Parr, R. G. *Phys. Rev. B* **1988**, *37*, 785−789.
(85) Stephens, P. J.; Devlin, F. J.; Chabalowski, C. F.; Frisch, M. J. *J. Phys. Chem.* **1994**, *98*, 11623−11627.
(86) Weigend, F.; Ahlrichs, R. *Phys. Chem. Chem. Phys.* **2005**, *7*, 3297−3305.
(87) Rappoport, D.; Furche, F. *J. Chem. Phys.* **2010**, *133*, 134105/1−134105/11.
(88) Häser, M.; Ahlrichs, R. *J. Comput. Chem.* **1989**, *10*, 104−111.
(89) Weigend, F.; Häser, M. *Theor. Chem. Acc.* **1997**, *97*, 331−340.
(90) Sierka, M.; Hogekamp, A.; Ahlrichs, R. *J. Chem. Phys.* **2003**, *118*, 9136−9148.
(91) *TURBOMOLE V6.4 2012*, a development of University of Karlsruhe and Forschungszentrum Karlsruhe GmbH, 1989−2007, TURBOMOLE GmbH, since 2007; available from http://www.turbomole.com.
(92) Ishii, K.; Hatanak, M.; Ueda, I. *Chem. Pharm. Bull.* **1991**, *39*, 3331−3334.
(93) Kurz, D.; Reinhold, J. *J. Mol. Struct. (THEOCHEM)* **1999**, *492*, 187−196.
(94) Frija, L. M. T.; Reva, I.; Ismael, A.; Coelho, D. V.; Fausto, R.; Cristiano, M. L. S. *Org. Biomol. Chem.* **2011**, *9*, 6040−6054.
(95) Cristiano, M. L. S.; Johnstone, R. a. W. *J. Chem. Res.* **1997**, 164−165.
(96) Dankwardt, J. W. *J. Org. Chem.* **1998**, *63*, 3753−3755.
(97) X-ray analysis revealed two polymorph structures of a $L_4Cu_4I_4$ complex (**5-I(b)** and **5-I(b)′**). They can be seen in Figure 2 and in Figure S1 in the Supporting Information
(98) Due to the low solubility of this complex in most organic solvents, which hampers purification by reprecipitation or recrystallization, a highly accurate elemental analysis cannot be achieved.
(99) Due the low solubility of complex **7-I(b)** and due to dissociation reactions seen in the emission spectra of complex **8-I**, these complexes were not further investigated for their behavior in different environments.
(100) Makal, A.; Benedict, J.; Trzop, E.; Sokolow, J.; Fournier, B.; Chen, Y.; Kalinowski, J. a; Graber, T.; Henning, R.; Coppens, P. *J. Phys. Chem. A* **2012**, *116*, 3359−3365.
(101) Liu, Z.; Djurovich, P. I.; Whited, M. T.; Thompson, M. E. *Inorg. Chem.* **2012**, *51*, 230−236.
(102) Krylova, V. A.; Djurovich, P. I.; Aronson, J. W.; Haiges, R.; Whited, M. T.; Thompson, M. E. *Organometallics* **2012**, *31*, 7983−7993.
(103) Lees, A. J. *Coord. Chem. Rev.* **1998**, *177*, 3−35.
(104) Tsuboyama, A.; Iwawaki, H.; Furugori, M.; Mukaide, T.; Kamatani, J.; Igawa, S.; Moriyama, T.; Miura, S.; Takiguchi, T.; Okada, S.; Hoshino, M.; Ueno, K. *J. Am. Chem. Soc.* **2003**, *125*, 12971−12979.
(105) Itokazu, M. K.; Polo, A. S.; Iha, N. Y. M. *J. Photochem. Photobiol. A: Chem.* **2003**, *160*, 27−32.
(106) Blasse, G.; Copper, O.; McMillin, D. R.; Lafayette, W. *Chem. Phys. Lett.* **1980**, *70*, 4−6.
(107) Deaton, J. C.; Switalski, S. C.; Kondakov, D. Y.; Young, R. H.; Pawlik, T. D.; Giesen, D. J.; Harkins, S. B.; Miller, A. J. M.; Mickenberg, S. F.; Peters, J. C. *J. Am. Chem. Soc.* **2010**, *132*, 9499−9508.